Journal of Geoscience and Environment Protection, 2025, 13(12), 116-129
https://www.scirp.org/journal/gep
ISSN Online: 2327-4344
ISSN Print: 2327-4336

Characteristics and Main Controlling Factors of Low Permeability Reservoirs in E_3s^2 of A Oilfield, Bohai Bay Basin

Junshou Zhao, Yanan Xu, Qiang Sun, Junliang Zhou, Xin Yang

CNOOC China Limited, Tianjin Branch, Tianjin, China
Email: zhaojsh9@cnooc.com.cn

How to cite this paper: Zhao, J. S., Xu, Y. N., Sun, Q., Zhou, J. L., & Yang, X. (2025). Characteristics and Main Controlling Factors of Low Permeability Reservoirs in E_3s^2 of A Oilfield, Bohai Bay Basin. *Journal of Geoscience and Environment Protection, 13,* 116-129.
https://doi.org/10.4236/gep.2025.1312007

Received: October 25, 2025
Accepted: December 2, 2025
Published: December 5, 2025

Abstract

The Second Member of the Shahejie Formation in A oilfield, Bohai Bay Basin, contains typical medium-low porosityand low permeability tight sandstone reservoirs. To study the features (petrology, porosity and physical properties) and forming mechanism of the target reservoirs, a series of experimental data were used, including cores observation, casting section identification, electron microscope observation and X-ray diffraction, combining with the theory of sedimentary petrology, reservoir sedimentology. The results show that the reservoir is porous reservoir featuring in middle composition and texture maturity, lithic arkoses, secondary dissolution porosity and I type of pore structure. The forming mechanisms of the reservoirs include sedimentation and diagenesis. Sedimentary facies are mainly by braid river deltas front sub-facies, the microfacies of underwater distributary channel have the best reservoir physical property and oiliness, easily forming favorable reservoirs. Particle size and the content of matrix are controlled by sedimentary hydrodynamic in different kinds of microfacies, then the best reservoirs are the coarse grained sandstone which have low matrix content. Primary pores in the reservoirs were almost killed by compaction and the cementation of carbonate cements and clay minerals, paulopost solution created secondary pores which are the mainly reservoir space. But the dissolution is not so strong that reservoirs still have low permeability. Therefore, secondary pores area in underwater distributary channel is the most favorable area for reservoirs to develop.

Keywords

Sedimentation, Diagenesis, Low Permeability Reservoir, A Oilfield, Bohai Bay Basin

1. Introduction

The A Oilfield in the Bohai Bay Basin is located at the western end of the Bonan Low Uplift in the Bohai Bay Basin, at the boundary of three major oil-generating enrichment zones: the Bozhong Sag, the Huanghekou Sag. It covers a total exploration area of approximately 30 km^2 (**Figure 1**), extending in a northeast direction. As a faulted anticline structure bounded by two boundary faults, it serves as a favorable site for oil and gas accumulation and is the first pilot test oilfield for low-permeability fracturing exploitation in the Bohai Sea (Liao et al., 2015). The sandstone reservoirs of the second and third members of the Shahejie Formation (E_3s^2 and E_3s^2) in the Paleogene are the main oil-bearing sequences of the oilfield, characterized by great burial depth, large trap area, and high closure amplitude, thus exhibiting considerable exploration potential. Previous studies (Xiao et al., 2025; Deng et al., 2007; Yang et al., 2025; Xue et al., 2025; Liu et al., 2025; Li, 2003; Xie et al., 2001; Yang et al., 2000; Yang et al., 2010) have been conducted on the sedimentary environment, provenance, and reservoir characteristics of the Shahejie Formation in the study area. These studies suggest that the E_3s^2 Member, influenced by dual provenances from the southwest and northwest, is dominated by medium-fine-grained lithic arkose deposited in the braided river delta front. Reservoir distribution shows certain diversity across different sedimentary periods, facies belts, and provenance directions, with overall low permeability. However, there is a lack of systematic research on the main controlling factors of reservoirs and the genesis of high-quality reservoirs in the study area, which fails to meet the needs of optimizing the oilfield's potential areas and deploying adjustment wells. Therefore, this study utilizes drilling core observation, thin-section identification, scanning electron microscopy (SEM), X-ray diffraction (XRD), capillary pressure curves, and other relevant analytical data to conduct a systematic investigation into the main controlling factors and formation mechanisms of low-permeability reservoirs in the E_3s^2 member of the study area. This research provides a geological basis for the subsequent pilot experiments and potential tapping of the oilfield.

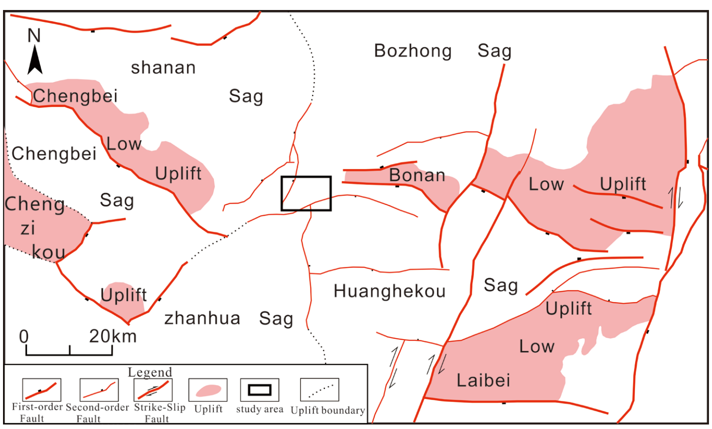

Figure 1. Location of study area.

2. Petrological Characteristics of the Reservoir

Based on the analysis of 101 sandstone samples in the study area, the reservoir of the E_3S^2 Member of the Shahejie Formation is mainly composed of medium-fine-grained lithic arkose (**Figure 2**). Microscopic identification and statistical analysis of clastic components show that the average content of quartz is 50.27%, feldspar (dominated by potassium feldspar) is 33.06%, and lithic fragments (mainly magmatic rock fragments, with intrusive rocks as the primary type) is 14.30%. Analysis of SEM and XRD data indicates that the average content of interstitial materials is 2.36%. The cement is dominated by carbonate minerals, with common quartz overgrowth; the matrix is mainly composed of clay minerals.

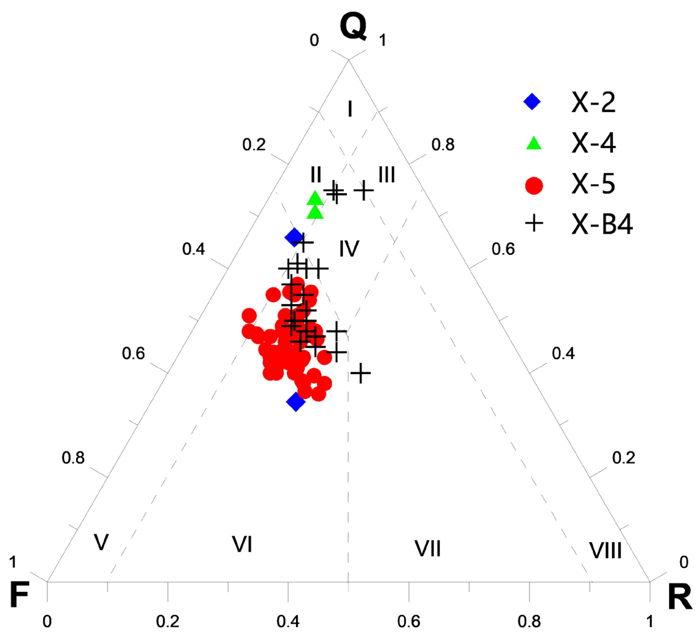

I. Quartz sandstone; II. Feldspathic quartz sandstone; III. Lithic quartz sandstone; IV. Feldspathic-lithic quartz sandstone; V. Feldspar sandstone; VI. Lithic arkose (or Lithic feldspar sandstone); VII. Feldspathic lithic sandstone; VIII. Lithic sandstone.

Figure 2. Triangular diagram of sandstone types of E_3s^2 in A oilfield.

Grain size analysis results show that the average particle size of the sandstone reservoir ranges from 0.05 to 0.33 mm, with a wide distribution (from argillaceous to gravel). Fine sandstone is the dominant type, accounting for 39.13%, followed by siltstone and medium sandstone. The sorting coefficient ranges from 1 to 2, the skewness ranges from 1.36 to 2.28 (showing extremely positive skewness), and the kurtosis varies within a narrow range of 5.15 to 7.59. Overall, the clastic particles exhibit good sorting, with subrounded-subangular rounding. The clastic particles are supported by a grain-supported structure, and the intergranular contact is mainly point-line or line contact. Compaction is strong in fine-grained sandstone, with local concave-convex contact observed; the cementation type is dominated by contact cementation. In summary, the sandstone reservoir has moderate compositional and textural maturity.

3. Pore and Physical Properties of the Reservoir

3.1. Pore Types

Observations of cast thin sections and SEM reveal that the intergranular spaces of the E_3S^2 sandstone reservoir are mostly filled with clay matrix and carbonate cement (Plate I-a), resulting in almost no primary pores. Secondary intergranular pores, formed by the dissolution of carbonate cement between clastic particles, are the dominant pore type, followed by intragranular pores formed by the dissolution of feldspar and lithic fragments. Moldic pores formed by the dissolution of ooids and bioclasts are occasionally observed. Fractures are rarely seen in cast thin sections and core observations; however, CT scanning reveals curved, embayed, and randomly distributed non-directional fractures (Plate I-b). These fractures are not seen penetrating the core, have a limited distribution, and are classified as non-conductive fractures. A small number of circular pores are observed around the fractures, suggesting that the fractures may be of dissolution origin.

3.2. Pore Structure

Mercury injection data of 53 sandstone samples from the E_3S^2 Member show the following average parameters: displacement pressure of 0.33 MPa, throat radius of 0.99 μm, saturation median radius of 1.00 μm, average pore-throat radius of 1.55 μm, maximum pore-throat radius of 14.96 μm, pore-throat sorting coefficient of 2.05, maximum mercury saturation of 83.99%, and mercury withdrawal efficiency of 29.44%. Through statistical analysis of the capillary pressure curve patterns and their characteristic parameters, the pore structure is roughly classified into two basic types (Figure 3).

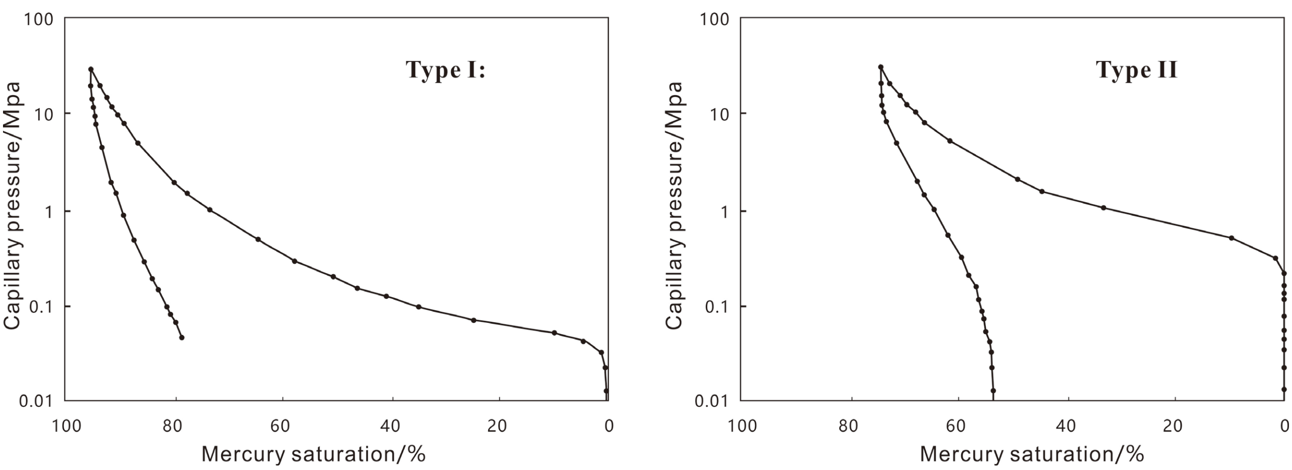

Figure 3. Typical capillary pressure curves of pore throat sandstones of of E_3s^2 in A oilfield.

Type I: Displacement pressure < 0.2 MPa, maximum mercury saturation > 80%, throat radius distribution > 1.0 μm. Characterized by relatively large throats, good sorting, and coarse skewness (fine throats), this type of reservoir has good physical properties and well-developed intergranular pores.

Type II: Displacement pressure ranging from 0.2 to 0.5 MPa, maximum mercury saturation ranging from 60% to 80%, throat radius ranging from 0.25 to 1.0 μm. Characterized by fine throats, poor sorting, and coarse skewness (extra-fine throats), this type of reservoir has poor physical properties.

3.3. Physical Properties

Statistical analysis of sample physical properties shows that the porosity ranges from 3.73% to 22.30% (average: 13.67%), and the permeability ranges from 0.0001 to 774.08 × 10^{-3} μm^2 (average: 34.36 × 10^{-3} μm^2), indicating a medium-low porosity and low permeability reservoir. The physical properties gradually deteriorate with increasing depth, and there is a good positive correlation between porosity and permeability (**Figure 4**). This suggests that the seepage channels of the E_3S^2 Member in this area are mainly pore-related reservoir spaces, less affected by fractures, and thus the reservoir is a porous reservoir dominated by matrix pores.

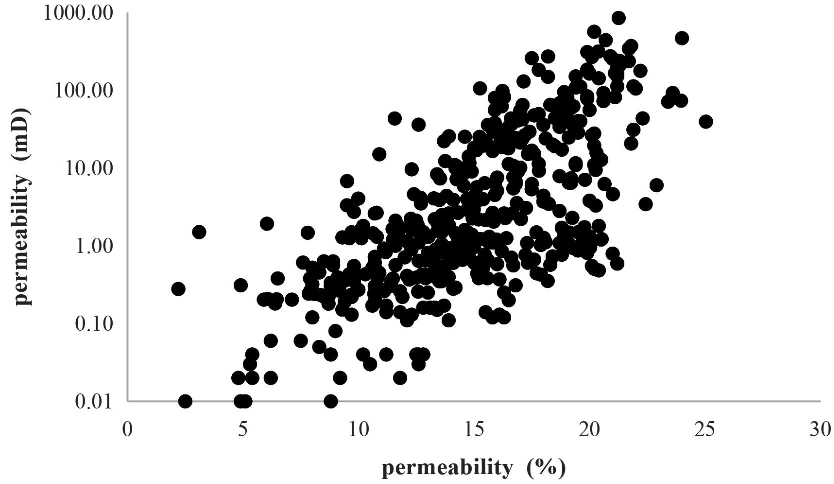

Figure 4. Porosity and permeability of reservoirs of E_3s^2 in A oilfield.

4. Formation Mechanism of Low-Permeability Reservoirs

4.1. Sedimentation

Sedimentation not only controls macro-factors such as reservoir scale and 3D distribution but also determines micro-factors (e.g., sediment particle size, matrix content, and rock composition) through hydrodynamic conditions of different sedimentary facies belts. These factors further affect the development of primary pores and permeability differences in the reservoir. Therefore, sedimentation is the inherent material basis and internal factor controlling reservoir physical properties (Jiang et al., 2004; Wen et al., 2007; Hu et al., 2013; Bloch et al., 2002).

The E_3S^2 reservoir in the study area was deposited in a braided river delta front and shore-shallow lake environment, including microfacies such as subaqueous distributary channels, mouth bars, interdistributary bays, shore-shallow lake beach bars, and shore-shallow lake mud (Figure 5). Among these, the subaqueous distributary channel microfacies in the delta front has the best physical properties, serving as a favorable sedimentary site for reservoir development (Table 1).

Table 1. The porosity and permeability of E_3s^2 microfacies in A oilfield.

sedimentary micro	samples	Porosity (%)		Permeability (mD)	
		average	range	average	range
subaqueous distributary channel	152	16.43	4.50 - 24.00	57.02	0.005 - 466.50
channel edge	41	13.42	4.80 - 21.20	0.51	0.02 - 4.30
estuary dam	6	8.93	5.40 - 12.60	0.09	0.006 - 0.43
beach-bar	7	10.25	4.60 - 26.30	0.65	0.01 - 4.72

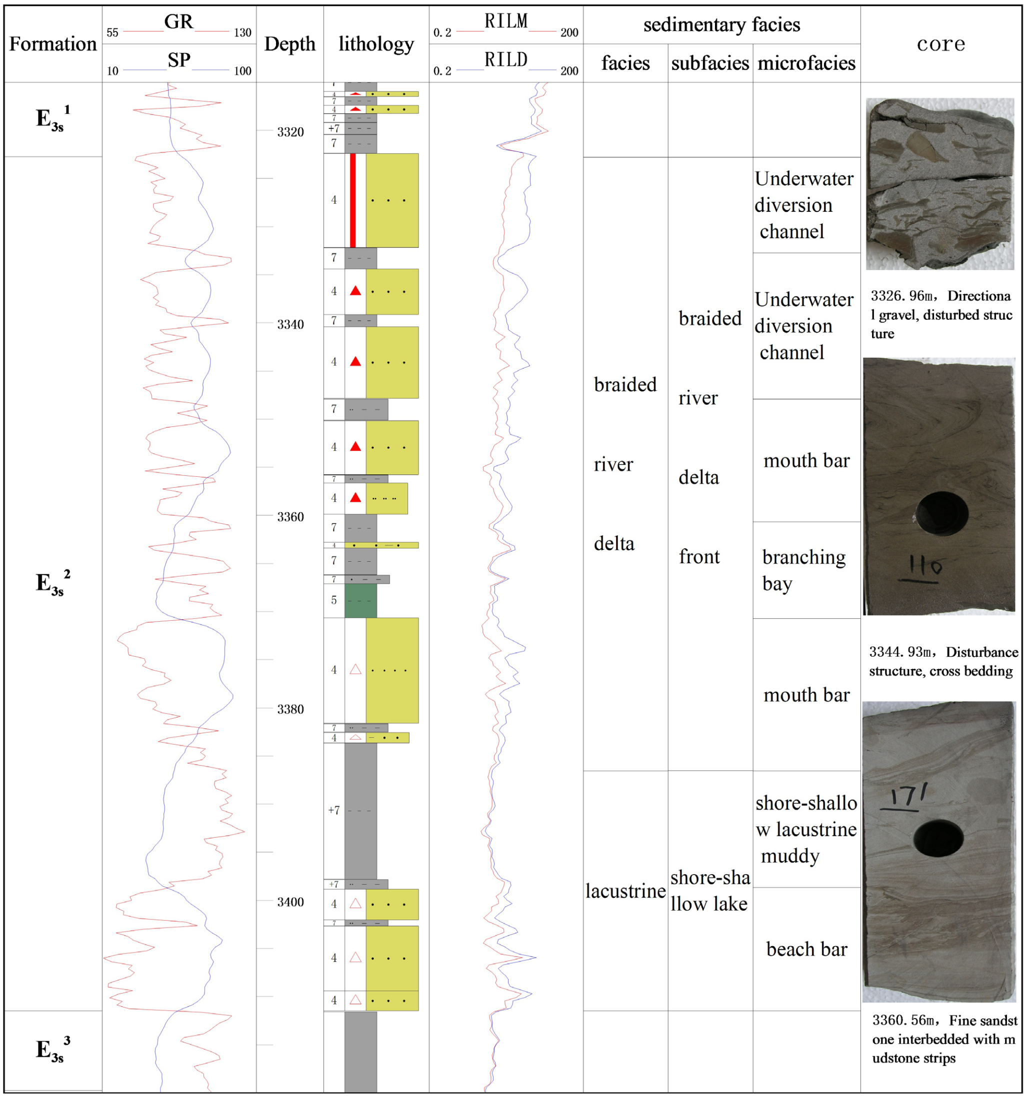

Figure 5. Characteristics of sedimentary microfacies of E_3s^2 in A oilfield.

As shown in **Figure 5**, the subaqueous distributary channel microfacies is dominated by gray medium-fine-grained lithic arkose; the sand bodies are mostly deposited in positive rhythms, with parallel bedding and cross-bedding developed. Gravel imbricate arrangement is visible at the bottom of positive rhythmic sand bodies, and the logging curve shape is box-like or bell-like, with comprehensive logging interpretation indicating mostly oil layers. Local intervals show composite rhythms of superimposed positive and reverse rhythms, reflecting the sedimentary process of delta channel sand bodies advancing and eroding early mouth bars. The beach bar microfacies is mainly composed of dark gray mudstone intercalated with sandy strips and thin-layer siltstone, with wavy cross-bedding developed; the logging curve shape is often serrated funnel-like or wide symmetric finger-like, with comprehensive logging interpretation indicating mostly oil-water layers or water layers. The interdistributary bay microfacies is dominated by argillaceous deposits, with the worst physical properties, making it difficult to form favorable reservoirs. Comprehensive analysis shows that the subaqueous distributary channel microfacies has better porosity, permeability, and oil-bearing property than other sedimentary microfacies, serving as the most favorable reservoir development zone in the area. Sedimentary microfacies macroscopically control the 3D distribution of primary reservoir physical properties.

Grain size analysis and thin-section observation show that reservoir physical properties tend to improve with increasing clastic particle size and decreasing matrix content (**Table 2**). Larger clastic particles indicate stronger sedimentary hydrodynamic conditions, which facilitate repeated washing and rounding of coarse clastic particles, resulting in good sorting, high rounding, and low matrix content-providing favorable conditions for the preservation of primary pores or subsequent diagenetic modification (Lin et al., 2014; Xu et al., 2015). Therefore, the clastic particle size and matrix content (controlled by sedimentary hydrodynamic conditions) have a significant impact on the physical properties of the reservoir in the study area.

Table 2. The porosity and permeability of E_3s^2 lithology in A oilfield.

lithology	samples	Porosity (%)		Permeability (mD)	
		average	range	average	range
Coarse sandstone	6	13.92	8.97 - 19.73	172.92	1.94 - 774.08
Medium-grained sandstone	32	13.15	5.15 - 18.87	23.46	0.33 - 277.86
Fine sandstone	24	12.33	6.96 - 17.83	0.85	0.04 - 6.61
very fine sandstone	7	13.40	10.80 - 16.00	0.81	0.24 - 2.00

4.2. Diagenesis

Diagenesis occurs throughout the process of sediment consolidation into rock, further modifying the inherent reservoir physical properties formed by sedimentation. It is the acquired condition and external factor controlling reservoir physical properties. Vitrinite reflectance (R_0) data show that the E_3s^2 Member has entered the low-maturity evolution stage, with R_0 concentrated in the range of 0.67% to 0.70%. The spore-pollen color is orange-yellow, with a thermal alteration index (TAI) of 2.5 to 2.6. The maximum pyrolysis temperature (Tmax) is mainly distributed between 423 and 437˚C (average: 432˚C). Authigenic clay minerals are dominated by illite, with an average relative content of montmorillonite in illite-smectite (I/S) mixed layers of 20%, indicating a high degree of I/S evolution (ordered mixed layer zone). According to the diagenetic stage division standard for clastic rocks, the diagenesis of the E_3S^2 Member is mainly in the middle diagenetic stage A. Combined with microscopic observation and previous research results (Sun et al., 2014), the diagenetic evolution sequence of the reservoir can be summarized as follows (**Figure 6**): compaction → early calcite precipitation → organic acid production → dissolution → secondary pores, authigenic kaolinite, authigenic quartz → illite precipitation → late ankerite filling and replacement. Based on their impact on reservoir porosity and permeability, diagenetic processes can be divided into destructive diagenesis (compaction, cementation) and constructive diagenesis (dissolution).

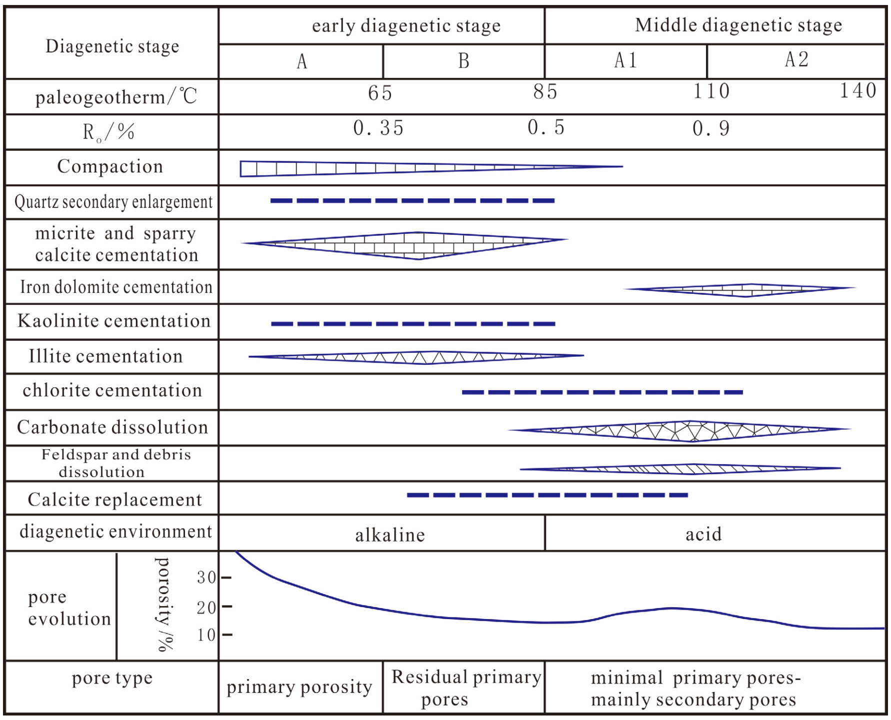

Figure 6. Diagenesis evolution sequence of E_3s^2 reservoirs in A oilfield.

1) Compaction

The sandstone reservoir in the study area has a burial depth of −3150 to −3300 m. Compaction is one of the main processes reducing reservoir porosity. With increasing burial depth, the effective stress of the overlying strata gradually increases, leading to a corresponding decrease in reservoir pore volume. As shown in the relationship diagram between sandstone cement content and negative cement porosity (Figure 7), almost all data points fall in the area dominated by compaction. Microscopic observation also reveals that the intergranular contact of clastic particles is mainly point-line or line contact (Plate I-c), followed by concave-convex-line contact; point contact is rare. Plastic clastic particles undergo plastic deformation (Plate I-d) and distortion, with partial pseudomatrix formation. Therefore, compaction is relatively strong, making it difficult to preserve primary pores.

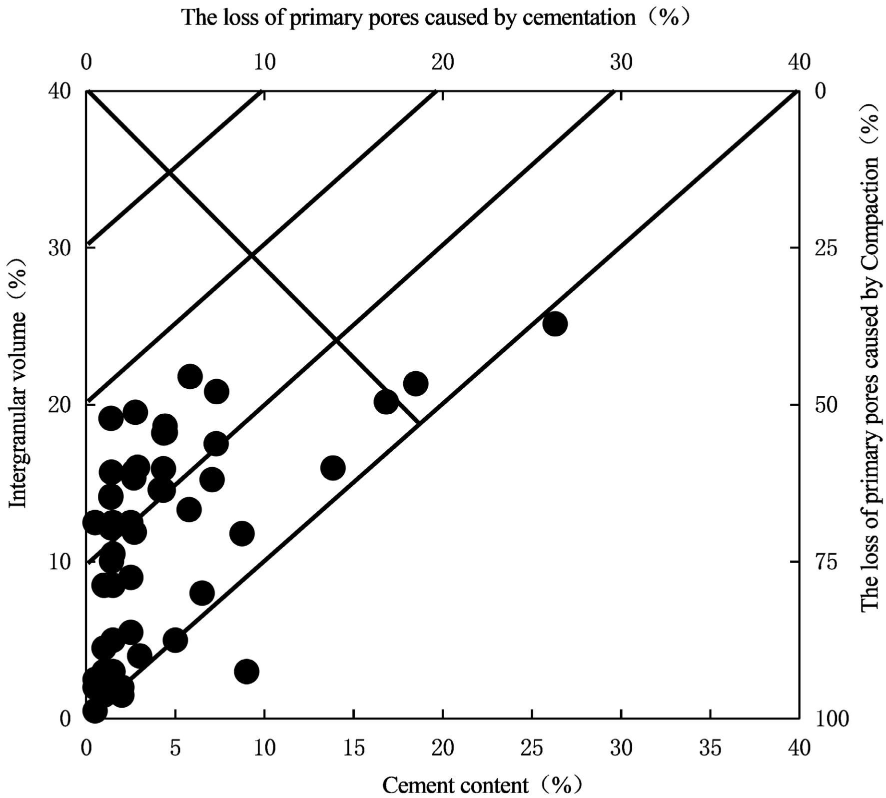

Figure 7. The relationship between compaction and cementation as factors controlling the porosity evolution of sample analysisde.

2) Cementation

a) Carbonate Cementation: During the deposition of the E_3S^2 Member, the study area had a shallow sedimentary water body, high salinity, and an alkaline diagenetic environment (Yang et al., 2010), leading to widespread carbonate cementation. The average content of carbonate cement is 8.15%, mainly composed of calcite and dolomite. Syngenetic micritic calcite cementation is strong (Plate I-e), forming micritic rims and pore filling; early diagenetic sparry calcite fills pores, forming a matrix-supported cementation. Affected by both compaction and carbonate cementation, primary pores in the early diagenetic stage are difficult to preserve, which significantly reduces the reservoir space.

b) Siliceous Cementation: Siliceous cementation is mainly manifested as quartz overgrowth and intergranular siliceous cement. Quartz overgrowth in the study area is commonly observed under thin-section microscopy (Plate I-f). SEM data show that intergranular siliceous cement locally develops into regularly shaped quartz crystals; some authigenic quartz microcrystals grow on the surface of quartz particles, continuously occupying part of the reservoir space and deteriorating reservoir physical properties (Plate I-g). Meanwhile, the presence of siliceous cement can also enhance the compaction resistance of the sandstone reservoir to a certain extent, exerting a constructive effect on reservoir physical properties.

c) Clay Mineral Cementation: SEM and XRD data show that clay mineral cementation generally deteriorates reservoir physical properties with increasing clay mineral content (**Figure 8**). The clay minerals in the E_3S^2 reservoir are dominated by illite (average relative content: 67%), with kaolinite, chlorite, and I/S mixed layers also present. During diagenesis, clay minerals often transform due to changes in temperature, pressure, or the fluid medium they contact. Smectite is transformed into illite through the process of potassium enrichment, aluminum enrichment, desilication, and dehydration, under the interaction with potassium-rich mineral dissolution and pore water. In an alkaline diagenetic environment with potassium feldspar, kaolinite also transforms into illite (Plate I-h), with the simplified reaction formula as follows:

$$2Al_2Si_2O_5(OH_4) + 2K^+ + OH^- \rightarrow 2KAl_3Si_3O_{10}(OH)_2 + 5H_2O$$

Ultimately, illite coats the particle surface in the form of fragments or scales, or divides intergranular pores in a pore-bridging manner (in the form of filaments (Plate I-i) or flakes), increasing the tortuosity and blocking throats, thereby deteriorating reservoir physical properties (Plate I-j).

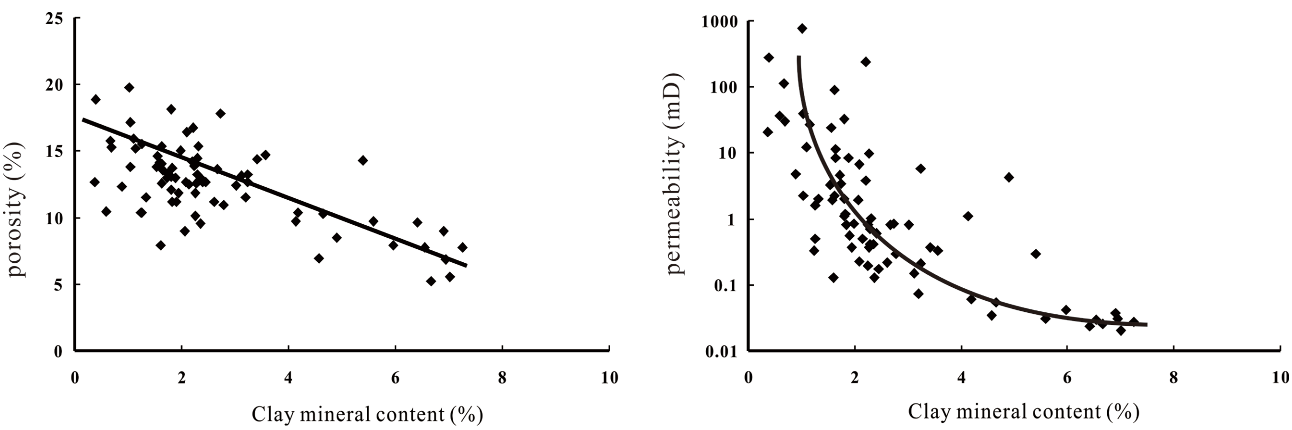

Figure 8. The relationship between content of clay minerals and petrophysical properties of E_3s^2 in A oilfield.

3) Dissolution

In a specific diagenetic environment, any clastic particles, matrix, cement, and replacement minerals in clastic rocks—including the most stable quartz and siliceous cement—can undergo dissolution to varying degrees (Jiang, 2003). The intensity of dissolution depends on the properties (pH, Eh, temperature, chemical composition, etc.) and quantity of fluids passing through the rock, as well as the stability and permeability of rock components. The rock type in the study area is mainly lithic arkose, with soluble carbonate cement developed in the interstitial materials, providing a favorable material basis for later dissolution. Cast thin-section data show that dissolution mainly occurs in intergranular carbonate cement, followed by the dissolution of feldspar and lithic fragments (Plate I-k, l). The main reason is that the burial depth of the study area is approximately 2400 meters. During the maturation of organic matter in source rocks, organic acids are released, which induce dissolution along the edges of soluble minerals (feldspar and lithic grains), grain fracture cracks, cleavage cracks, and the hydrochloride cements between clastic grains. This dissolution leads to the development of expanded intergranular pores, reduced intergranular pores, intragranular pores, and moldic pores are observed; however, the overall dissolution intensity is weak, with no large-scale pores or super-large dissolved pores formed by dissolution. The absolute content of mixed pores is 3.86%, accounting for an average of 70% of the total pores; the absolute content of secondary pores is 1.55%, accounting for an average of 28% of the total pores. The reservoir pores are dominated by expanded intergranular pores, but their absolute content is low. This indicates that dissolution in the reservoir mainly acts on the cement between clastic particles; however, the limited dissolution intensity, while exerting a constructive effect on reservoir physical properties, cannot completely change the low-permeability characteristics of the reservoir.

5. Conclusion

1) The E_3S^2 reservoir of the A Oilfield is a typical medium-low porosity and low permeability sandstone reservoir, mainly composed of lithic arkose, with moderate compositional and textural maturity.

2) The impact of sedimentation on reservoir physical properties is as follows: larger clastic particle size and lower matrix content lead to better reservoir physical properties; the subaqueous distributary channel microfacies in the delta front subfacies has the best physical properties and significantly better oil-bearing property than other microfacies, with a relatively wide distribution, serving as a favorable sedimentary site for reservoir formation; the mouth bar and beach bar microfacies have relatively poor physical properties and oil-bearing property; the interdistributary bay microfacies is mostly argillaceous deposits, making it difficult to form reservoirs.

3) The impact of diagenesis on reservoir physical properties is mainly reflected in: compaction makes it difficult to preserve primary pores; carbonate cementation and clay mineral cementation in the cementation process lead to the almost complete disappearance of primary pores; although siliceous cementation reduces reservoir physical properties, it can also reduce the damage of compaction to reservoir physical properties to a certain extent, exerting a dual effect on reservoir physical properties. Secondary dissolution is the main way to increase pores in the

later stage, but its limited intensity cannot completely change the medium-low porosity and low permeability characteristics of the reservoir. Therefore, compaction, carbonate cementation, and clay mineral cementation are the main factors leading to low permeability of the reservoir in this area; the subaqueous distributary channel microfacies and carbonate dissolution facies zone are favorable areas for reservoir development, serving as preferred targets for future adjustment well targeting. Furthermore, the distribution pattern of subaqueous distributary channels should be taken into account in hydraulic fracturing design.

Conflicts of Interest

The authors declare no conflicts of interest regarding the publication of this paper.

References

Bloch, S., Lander, R. H., & Bonnell, L. (2002). Anomalously High Porosity and Permeability in Deeply Buried Sandstone Reservoirs: Origin and Predictability. *AAPG Bulletin, 86,* 301-328.

Deng, Y., & Li, J. (2007). Breakthroughs of Geological Concepts in Exploration and Evaluation of BZ25-1 Field. *Petroleum Exploration and Development, 34,* 646-652.

Hu, M., Shen, J., & Hu, D. (2013). Reservoir Characteristics and Its Main Controlling Factors of the Pinghu Formation in Pinghu Structural Belt, Xihu Depression. *Oil & Gas Geology, 34,* 16-173.

Jiang, L., Gu, J., & Guo, B. (2004). Characteristics and Mechanism of Low Permeability Clastic Reservoir in Chinese Petroliferous Basin. *Acta Sedimentologica Sinica, 22,* 13-18.

Jiang, Z. (2003). *Sedimentology* (pp. 157-158). Petroleum Industry Press.

Li, L. (2003). The Diagenesis Model of Tertiary Sandstone Reservoir in Bozhong Area. *China Offshore Oil and Gas: Geology, 17,* 359-364.

Liao, X., Liu, Q., Li, C. et al. (2015). Distribution of the Present Stress in Low Permeability Oilfield of Bozhong 25-1 and Its Effect on Development. *Journal of Geomechanics, 21,* 30-31.

Lin, X., Liu, L., Tian, J. et al. (2014). Characteristics and Controlling Factors of Tight Sandstone Reservoirs in the 5th Member of Xujiahe Formation in the Central of Western Sichuan Depression. *Oil & Gas Geology, 35,* 224-230.

Liu, Z., Zhu, X., Liu, G. et al. (2025). Study on the Difference of Petroleum Accumulation Between Paleogene and Neogene in the Western Bozhong Sag, Bohai Bay Basin. *Lithologic Reservoirs, 37,* 78-89.

Sun, H., Li, C., Zhong, D. et al. (2014). Characteristics and Origin of Low Pemeability Reseroir of the Third Member of Shahejie Fomation in Bozhong 25-1 Oimeld. *Lithologic Reservoirs, 26,* 11-16.

Wen, H., Zheng, R., Chen, H. et al. (2007). Characteristics of Chang 6 Sandstone Reservoir in Baibao-Huachi Region of Ordos Basin. *Acta Petrolei Sinca, 28,* 46-51.

Xiao, D., Fan, T., Yang, E. et al. (2025). Microscopic Pore Structure Characteristics and Multi-Dimensional Parameter Classification Evaluation of Low-Permeability Reservoirs in the Shahejie Formation, Bozhong Oilfield. *Special Oil & Gas Reservoirs, 32,* 41-49.

Xie, W., Deng, H., Wang, H. et al. (2001). Palaeogene Reservoir Rocks in Central Bohai Gulf Depression and Their Controls. *Sedimentary Geology and Tethyan Geology, 15,* 111-119.

Xu, M., He, Z., Yin, W. et al. (2015). Characteristics and Main Controlling Factors of Tight Sandstone Reservoirs in the 8th Member of The Yanchang Formation in Zhenjing Area, Ordos Basin. *Oil & Gas Geology, 36,* 240 -247.

Xue, Y., Yang, H., Huang, Z. et al. (2025). New Recognition of Hydrocarbon Accumulation and Enrichment and Discovery of Large-Scale Oil and Gas Fields in Bohai Sea Area, Bohai Bay Basin. *China Petroleum Exploration, 30,* 58-69.

Yang, H., Fang, Z., Wang, F., Jiang, F., Qi, Z., Liu, M., Zheng, X., Chen, D., & Hu, T. (2025). Influence of Deep Hydrothermal Fluid on Organic Matter Enrichment and Its Activity Mode in Shahejie Frmation and Dongying Formation of Bohai Bay Basin. *Acta Ptrolei Sinica, 46,* 1089-1107.

Yang, X., Chen, H., Ye, J. et al. (2000). Large Lake Deltas and Their Hydrocarbon Potential in Bozhong Sag. *China Offshore Oil and Gas: Geology, 14,* 226-232.

Yang, Y., Pan, F., Tian, H. et al. (2010). Characteristics and Classif Ication and Evaluation of Low Porosity and Permeability Reservoir in Shahejie Formation of BZ25-1 Oilfield. *Geoscience, 24,* 685-693.

Appendix

Plate Ⅰ

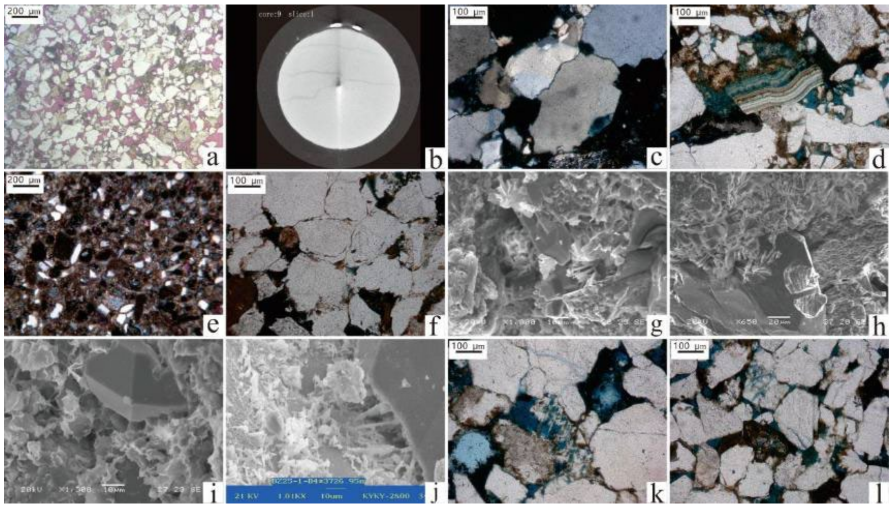

Explanation of Plate I: (a) Well X-5, 3334.80 m, sparry calcite cementation; (b) Well X-5, 3341.23 m, developed dissolution fractures; (c) Well X-B4, 3738.4 m, suture contact of clastic particles, (−) 10 × 10; (d) Well X-B4, 3733.6 m, bent deformation of biotite, (−) 10 × 10; (e) Well X-A13, 3367.12 m, intergranular argillaceous calcite cementation; (f) Well X-4, 3482.53 m, quartz overgrowth; (g) Well X-5, 3345.33 m, quartz overgrowth presenting as euhedral crystals; (h) Well X-5, 3341.84 m, flaky kaolinite in bundled aggregates attached to particle surfaces, with kaolinite transforming into flaky illite; (i) Well X-B4, 3723.20 m, hair-like illite; (j) Well X-B4, 3727.0 m, flaky illite dividing intergranular pores in a pore-bridging manner; (k) Well X-B4, 3738.4 m, intragranular pores formed by feldspar dissolution, (−) 10 × 10; (l) Well X-B4, 3731.90 m, (−) 10 × 10, developed primary pores, mixed pores and secondary pores, with mixed pores as the dominant type.